Interaction of angiogenic microvessels with the extracellular matrix

Laxminarayanan Krishnan,[1] James B. Hoying,[2] Hoa Nguyen,[1] Helen Song,[2] and Jeffrey A. Weiss[1]

[1]*Department of Bioengineering, University of Utah, Salt Lake City, Utah; and* [2]*Division of Microcirculation, Arizona Research Laboratories, University of Arizona, Tucson, Arizona*

Krishnan L, Hoying JB, Nguyen H, Song H, Weiss JA. Interaction of angiogenic microvessels with the extracellular matrix. *Am J Physiol Heart Circ Physiol* 293: H3650–H3658, 2007. First published October 12, 2007; doi:10.1152/ajpheart.00772.2007.—The extracellular matrix (ECM) plays a critical role in angiogenesis by providing biochemical and positional cues, as well as by mechanically influencing microvessel cell behavior. Considerable information is known concerning the biochemical cues relevant to angiogenesis, but less is known about the mechanical dynamics during active angiogenesis. The objective of this study was to characterize changes in the material properties of a simple angiogenic tissue before and during angiogenesis. During sprouting, there was an overall decrease in tissue stiffness followed by an increase during neovessel elongation. The fall in matrix stiffness coincided with peak matrix metalloproteinase mRNA expression and elevated proteolytic activity. An elevated expression of genes for ECM components and cell-ECM interaction molecules and a subsequent drop in proteolytic activity (although enzyme levels remained elevated) coincided with the subsequent stiffening. The results of this study show that the mechanical properties of a scaffold tissue may be actively modified during angiogenesis by the growing microvasculature.

biomechanics; matrix metalloprotease

ANGIOGENESIS, THE GROWTH OF new vasculature from existing blood vessels, is central to normal physiological and healing processes. Angiogenesis occurs by either intussusception, where the parent vessel splits into daughter vessels, or more commonly by endothelial cell (EC) sprouting from parent vessels. During angiogenesis, normally quiescent capillary ECs (1, 36) are stimulated to switch to an angiogenic phenotype (12). Angiogenic endothelial cells take on invasive and proliferative phenotypes, degrade the basement membrane, and invade the extracellular matrix (ECM) (25). These cells form new vessel sprouts that guide the growing neovessel through the ECM. Eventually, the neovessels mature with the development of pericyte coverage and form perfusion-capable capillary networks (15).

The ECM influences the process of angiogenesis through two mechanisms. The first is by acting as a biochemical regulator of EC phenotype. Considerable work has demonstrated the importance of outside-in signaling that occurs from the ECM via the integrins in ECs. For example, the ligation of the $\alpha_v\beta$-integrins is essential to prevent apoptosis in angiogenic ECs (11, 36). Also, matrix molecules, such as those comprising the basement membrane, decorin (DCN), and tenascin C (TNC), signal ECs to establish and maintain capillary-like structures during and following angiogenesis. ECM molecules such as hyaluronan can inhibit angiogenesis and reduce EC migration and adhesion (26). Finally, the ECM may indirectly regulate the phenotype of ECs by acting as a reservoir for bound growth factors and proteases, thereby affecting the bioavailability of these important biochemical signals. The second mechanism by which ECM can regulate angiogenesis is by serving as a structural framework to support sprout and neovessel structure and function. Matrix flexibility or stiffness is a significant modulator of metalloproteinase activity in ECs (39, 41). Metalloproteinase activity is an essential aspect of angiogenesis (32). In addition, matrix molecules, such as fibronectin (FN), may be responsible for inducing tissue alignment and providing architectural clues for the neovessels (9, 14). Finally, the ECM provides a foundation from which intracellular stresses, critical to EC function, are generated.

The invasive and proliferative activities of angiogenic ECs may have the propensity to influence the material properties of the ECM. ECs produce matrix metalloproteinases (MMPs)-2, -9, -13, and -14 that degrade the basement membrane and remodel the surrounding ECM to facilitate capillary ingrowth (23). Given how the ECM plays a central role in angiogenesis, the EC-dependent effects on ECM may, in turn, influence angiogenesis. However, little is known about this dynamic interaction between the ECM and angiogenic vessels and its impact on wound healing. A better understanding of this interaction will also lead to discerning the underlying mechanisms affecting the mechanical properties of healing or healed tissues, as well as facilitate the design of functionalized tissue-engineered constructs. The objective of this study was to investigate alterations in the mechanical properties of three-dimensional vascularized collagen constructs due to angiogenesis and to interpret these changes in the context of measurements of microvessel proliferation, proteolysis, and gene expression.

MATERIALS AND METHODS

In vitro model of angiogenesis. All animal protocols were approved by the University of Utah Institutional Animal Care and Use Committee. A three-dimensional model of angiogenesis was adapted for use in the present study (16). Rat microvessel fragments were isolated from epididymal fat pads of retired breeder Sprague-Dawley rats (>500 g). The pads were minced and subjected to limited digestion with 2 mg/ml of *Clostridium* collagenase (Worthington Biochemicals, Lakewood, NJ) and 2 mg/ml bovine serum albumin (BSA; Sigma-Aldrich, St. Louis, MO) in Dulbecco's cation-free phosphate buffered saline (DCF-PBS, pH 7.4) at 37°C. The digestion solution was centrifuged to obtain a pellet. The pellet was washed twice and resuspended in DCF-PBS containing 0.1% BSA and then sequentially filtered through 500-μm and then 30-μm sterile nylon membrane filters in a Cellector tissue sieve (Thermo EC, Milford, MA). The first

filtration step eliminates undigested particulate debris, and the second step retains larger vessel fragments of interest, while allowing single cells and smaller fragments to pass through. The 30-μm membrane was flushed with 0.1% BSA DCF-PBS, and the fragments were collected in a sterile Petri dish. Forty microliters of this suspension were pipetted on a glass slide, and the fragments were counted systematically throughout the entire drop. The final yield of fragments in the suspension volume was determined from an average of at least two such counts. The suspension was then centrifuged to obtain a pellet of rat fat microvessel fragments. Fragments consist of arterioles, venules, and capillaries with abluminally associated smooth muscle cells and pericytes (16).

Sterile rat tail collagen type I (Discovery Labware, BD Biosciences, Bedford, MA) was mixed with filter-sterilized Dulbecco's modified Eagle medium (DMEM, GIBCO-Invitrogen, Carlsbad, CA) to yield final concentrations of 3 mg/ml of collagen in 1× DMEM. Microvessels were suspended in the collagen solution at 15,000 fragments/ml; 1.1–1.5 ml of this suspension were pipetted into custom culture chambers and polymerized at 37°C and 95% humidity for 30 min (Fig. 1) (20). The custom chambers have fixed anchors near one end and a mobile post near the other end with holes (1-mm diameter) to allow the collagen solution to pass through. There is a reservoir of media at one end, which is blocked during polymerization. Gels are overlaid with 1× DMEM containing 10% (vol/vol) fetal bovine serum (Intergen, Purchase, NY) and incubated until time for mechanical testing or RNA extraction. Approximately 30% of the media was changed on the 3rd day of culture and every other day thereafter. Cultures for mechanical testing and RNA extraction were used on *days 1*, *6*, and *10*, during which the gels contracted from the sides of the chamber (Fig. 1).

Viscoelastic testing of vascularized gels. Dynamic viscoelastic testing was carried out using a piezoelectric actuated test system (Fig. 2) and our established protocol (20). Twenty-four vascularized gels and 15 native gels (no vessels) were tested. Eight vascularized gels each were tested at *day 1*, *day 6*, and *day 10* of culture, while six, four, and five native gels polymerized from the same collagen were tested at the same culture periods.

To quantify changes in geometry, construct cross-sectional areas were measured at the middle third, and an average of multiple measurements was used. The cross-sectional area of each vascularized construct was normalized by that of the corresponding native gel [ratio of vascularized to native gel (V/N)] to obtain a normalized cross-sectional area for graphical display. A one-way ANOVA was
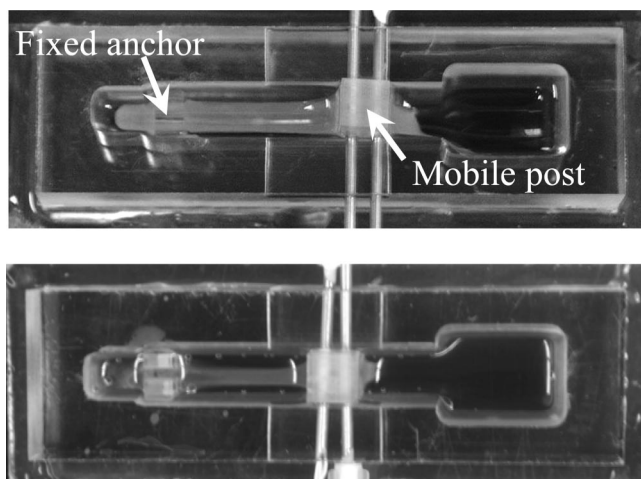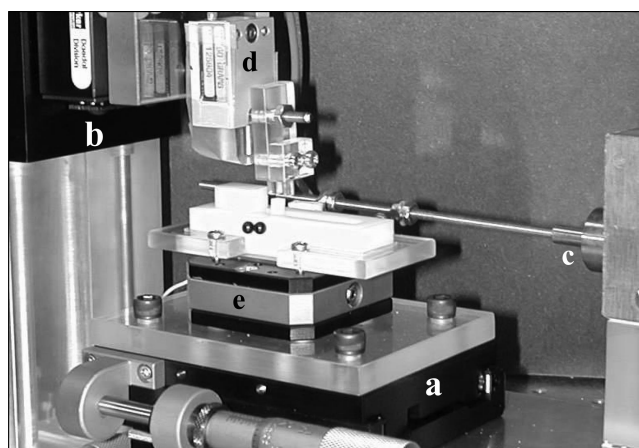

Fig. 2. Mechanical test device. a, *x-y* positioning stage; b, *z* positioning stage; c, linear variable differential transformer; d, load cell; e, piezoelectric stage.

used to test for any effect of culture time on the normalized cross-sectional area.

Gels were stretched between a fixed anchor post on the custom culture chamber and a mobile anchor interfaced to a load cell. The testing protocol consisted of preconditioning at 6% strain, followed by sinusoidal testing at three strain levels (2, 4, and 6%) and four strain rates (0.05, 0.1, 1, and 5 Hz). Viscoelastic properties of the constructs were calculated using the principles of linear viscoelasticity (13). Dynamic stiffness (M) and phase shift (ϕ) of the constructs were calculated as:

$$M = \frac{A_\sigma}{A_\varepsilon}; \quad \phi = \phi_\sigma - \phi_\varepsilon \qquad (1)$$

where (A_ε, ϕ_ε) and (A_σ, ϕ_σ) are the amplitudes and phases of the strain-time and stress-time data, respectively. The M represents the tangent modulus of the material for a particular strain rate and amplitude. The ϕ describes the lag in time between the stress and strain sine waves and is a direct measurement of energy dissipation by the material. For a purely elastic material, $\phi = 0$, indicating that the stress-time and strain-time signals are completely in phase, while for a fluid, $\phi = \pi/2$, indicating that the stress response leads the strain by 90°. Viscoelastic materials exhibit a phase angle between these two extremes.

The dynamic stiffness of the vascularized constructs was normalized to that of the native constructs at each culture time to compute V/N. The phase-shift difference of native gels was subtracted from that of the vascularized constructs at each culture time to compute a phase difference between vascularized and native gels (V − N). Multiple two-way ANOVAs were used to assess the effect of culture time and strain level for the individual test subsets and the normalized data. Kruskal-Wallis analysis was used when assumptions of normality or equal variance were violated.

Effects of MMP-9 on material properties of native collagen gels. The effect of MMP-9 on the material properties of native collagen gels was determined by viscoelastic testing of gels before and after the addition of MMP-9 to the media overlaying the gels. Mechanical testing of 16 native collagen gels was carried out 24 h after polymerization. Media in the chambers was then replaced with culture media containing 0.1% Thiomersal, penicillin-streptomycin (100 U/ml), and amphotericin B (0.25 μg/ml). MMP-9 activity on the substrate was verified by zymography. Activated human recombinant MMP-9 (67 kDa form, PF140, EMD Biosciences) was added to the media in eight of the chambers (4 μg per chamber), and the remaining eight gels were used as controls. Mechanical testing was repeated after 24 h. Multiple two-way repeated-measures ANOVAs were used to examine

Fig. 1. Custom culture chambers with vascularized constructs. *Top*: day 6 of culture. Contraction of gels away from the vessel wall was evident at *day 6*. *Bottom*: *day 10* of culture. By *day 10*, the constructs have contracted away from the chamber walls, but integrity with the anchor points was maintained.

the effect of test time and MMP-9 treatment on the mechanical properties of the gels.

Microvessel fragment density. Three gels each from *days 1* and *6* of culture and four gels from *day 10* of culture were analyzed for vessel density. Vascularized gels were fixed in 1% formalin and processed into paraffin. Five sections, 10 μm thick, were taken every eighth section, from the central one-third of the gel and mounted in paraffin. The sections were deparaffinized and stained with rodent endothelium-specific fluorescein-conjugated *Griffonia simplicifolia* (GS-1) lectin (Vector Laboratories, Burlingame, CA). The total numbers of GS-1-positive structures were counted at 4× magnification with a Nikon Diaphot inverted microscope. Four fields were evaluated per section, and the density expressed as the number of vessels per unit area (mm^2). The mean vessel density per unit area was evaluated from five sections per sample at each time point. One-way ANOVA was used to analyze the effect of culture time.

Proteolytic activity. Media and culture lysates were evaluated for gelatinolytic activity. MMP extraction was based on established protocols (6, 45). Collagen gels were weighed and homogenized (OMNI International, Marietta, GA) for 15 s in low-calcium Triton X buffer (10 mM CaCl$_2$ in 0.25% Triton X-100, 1 ml/200 mg tissue wet weight, Sigma-Aldrich). The homogenate was centrifuged for 30 min at 4°C, and the supernatant containing unbound MMPs was collected. The pellet was resuspended in high-calcium buffer (50 mM Tris·HCl, 100 mM CaCl$_2$, 0.15 M NaCl, pH 7.4), heated at 60°C for 6 min, and centrifuged for 30 min at 4°C to dissociate bound collagenases. Six vascularized and native gels were analyzed for proteolytic activity using the EnzCheck collagenase assay kit (Molecular Probes, Carlsbad, CA). Culture media was collected during periodic media changes and stored at −70°C, and pooled media was used for analysis. Fluorescence due to substrate lysis was quantified using a SynergyHT multiwell plate reader (Bio-Tek, Winooski, VT). *Clostridium* collagenase was used to generate a standard curve. Each reaction volume of 200 μl was made up of 10 μl of DQ-gelatin (1 mg/ml), 90 μl of buffer (50 mM Tris·HCl, 5 mM CaCl$_2$, pH 7.4), and 100 μl of clostridial collagenase, pooled media, or supernatants from tissue lysates or heat extractions. The reaction mix was incubated overnight at room temperature, and the fluorescence read after 12 h and expressed as average absolute units of activity in each subset (media and tissue lysates) per time point. The total genomic DNA in the tissue lysates was determined fluorometrically using the Quant-iT DNA assay kit (Molecular Probes, Eugene, OR). The total proteolytic activity of each sample (media and lysates) was normalized to the amount of DNA in the sample, and the activity was expressed as units per micrograms of DNA. One-way ANOVAs were used to analyze the effect of culture time.

Quantitative polymerase chain reaction. Six vascularized gels each were cultured for 1, 6, and 10 days. Additionally, pooled microvessel fragments equivalent to the number used for six gels were harvested to serve as *day 0* controls. Samples were stored in RNALater (Ambion, Austin, TX). RNA was extracted using a phenol-based protocol (24). Further processing was carried out in RNEasy MINI elute columns (Qiagen, Valencia, CA). RNA was eluted from the column in 52 μl of nuclease-free water. Two microliters of the solution were used to quantify RNA using Ribogreen (Molecular Probes-Invitrogen). The remaining RNA solution was treated with DNase I (Sigma-Aldrich) and then processed through an RNeasy MinElute cleanup kit (Qiagen). RNA was reverse transcribed to cDNA using the EndoFree RT kit (Ambion).

Primers (Biosearch Technologies, Novato, CA) were designed for 18 genes of interest and 5 housekeeping genes [GAPDH, hypoxanthine phosphoribosyltransferase, ubiquitin, dynactin 2, and YWH], covering the broad categories of MMPs [MMPs-2, -9, -13, membrane type 1 (MT1)-MMP] and their inhibitors [tissue inhibitor of MMP (TIMPs)-1 and -2]; growth factors [vascular endothelial growth factor (VEGF) and its receptor, basic FGF, bone morphogenic protein 1, platelet-derived growth factor (PDGF)]; matrix proteins (collagens 1, 3, and 8); and cell-matrix interaction proteins [DCN, TNC, FN, hyaluronic acid synthase (HAS)] using nucleotide sequences identified from the NCBI database and Primer3 (27). A Blast search was performed on the primer pairs to confirm target specificity. Polymerase chain reaction reactions were optimized individually with rat skeletal muscle cDNA as the template.

Quantitative polymerase chain reaction was carried out on a thermal cycler (RotorGene 3000, Corbett Research). Each 10-μl reaction consisted of UDG Supermix (Invitrogen), 1.5–6 mM primers (forward/reverse), SYBRgreen dye (Molecular Probes), and 5 μg cDNA, except in case of controls. Reactions were carried out in triplicate and grouped so that all samples for a specific target gene were analyzed in a single run. Reaction efficiency for each target was calculated from a standard curve of pooled cDNA. Expression efficiencies were calculated from a standard curve for each target. Relative expression levels were calculated using the method of Vandesompele et al. (40). Briefly, the best housekeeping genes that did not alter significantly over the experimental conditions were determined using the GeNorm software, and a normalization factor was calculated for each sample. The relative expression levels of these targets were the ratios of their raw expression levels to this normalization factor, allowing direct comparison of expression levels between both different treatment effects and different target genes. One-way ANOVAs were used to compare the normalized data for significant differences when the data were normally distributed. The Kruskall-Wallis test was used when data were not normally distributed.

MMP zymography. Six additional vascularized gels (2 each at *days 1*, *6*, and *10* of culture) were analyzed via MMP zymography to assess the presence of MMP-2 and MMP-9 protein. For each construct, the culture media were removed and saved at −20°C in 50-μl aliquots. Each gel was homogenized using a tissue homogenizer (Tissue Tearor, BioSpec Products, Bartlesville, OK) in 200 μl of zymography loading buffer [80 mmol/l Tris·HCl (pH 6.8), 4% SDS, 10% glycerol, and 0.01% bromophenol blue] and centrifuged at 12,000 rpm for 10 min in 1.5-ml microfuge tubes. The supernatants were removed and stored at −20°C. Equal amounts of protein (MicroBCA, Pierce, Rockford, IL) were separated by electrophoresis in a 0.75-mm SDS 7% PAGE gel containing 0.2% porcine gelatin. An additional lane was loaded with 2 μl of purified native MMP-2 and MMP-9 enzymes diluted 1:200 (Sigma) for each run to serve as migration standards. Following electrophoresis, SDS was removed by soaking in 75 ml of renaturing solution (2.5% Triton X-100) for 45 min. The gels were then preincubated in developing buffer [50 mmol/l Tris·HCl (pH 7.5) and 10 mmol/l CaCl$_2$] at room temperature for 30 min followed by incubation overnight at 37°C in fresh developing buffer to develop the zymogram. Zymograms were imaged with a digital camera using back illumination. Pixel intensities for select bands were determined from the images using the image analysis package Metamorph (Molecular Devices, Sunnyvale, CA).

RESULTS

In vitro model of angiogenesis. Angiogenesis began predictably on the 3rd day of culture, with ECs breaching the abluminal walls to form sprouts, both at the ends and midregions of parent vessels. Newly formed translucent EC cords were evident by the 6th day, progressing or regressing dynamically to ultimately form vascular networks by the 10th day (Fig. 3). The resulting microvessel networks, characterized previously (16, 33), have a collagen IV basement membrane, stain for von Willebrand factor, and integrate with host vessels after in vivo implantation (33).

Constructs contracted away from the chamber walls as early as the 6th day, resulting in decreases in cross-sectional areas (Fig. 4). There was a significant effect of culture time on the normalized cross-sectional area ($P < 0.001$). In particular, the
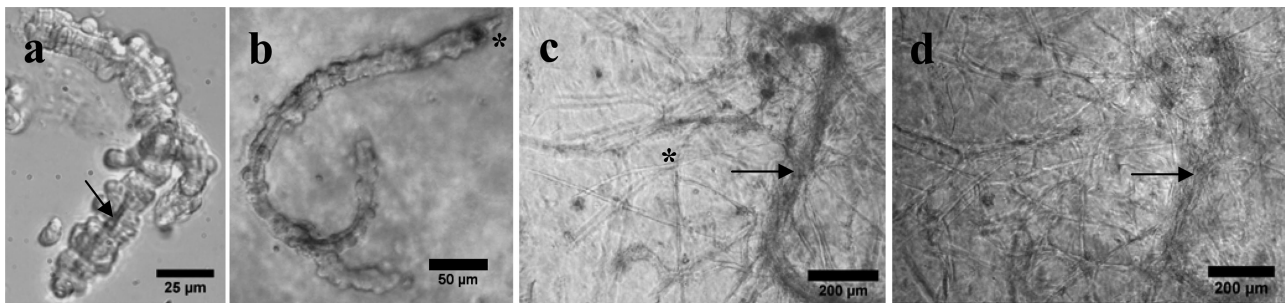
Fig. 3. Phase-contrast micrographs of rat microvessel fragments, illustrating representative microvessel sprouting and growth over time in cultures. *a*: Freshly isolated microvessel fragment showing lumen (arrow) and blood cells. *b*: Early sprout formation (*) at *day 1*. *c*: Translucent invading neovasculature at *day 7* (*), elongating into the collagen gel from parent vessel (arrow). *d*: Same field as *c*, showing well-formed vascular networks and anastamoses at *day 10*.

day 10 normalized cross-sectional area was significantly less than that at *days 1* and *6* ($P < 0.001$ in both cases).

Microvessel fragment density. Vessel density increased gradually from the 1st day to the 6th and 10th days of culture (Fig. 5). The vessel density at the 10th day was significantly higher than the density at the 1st ($P < 0.001$) and 6th days of culture ($P = 0.018$).

Mechanical properties of collagen gels. We sought to quantify changes in the mechanical properties of the vascularized constructs that occurred during angiogenesis. To accomplish this, we performed viscoelastic testing of vascularized and native gels at three different times during culture. In general, there was a strain level-dependent increase in dynamic stiffness for both vascularized as well as native constructs at all test times ($P < 0.001$). There was also a strain rate-dependent stiffening of the constructs (Fig. 6, *left*). The V/N for dynamic stiffness fell significantly ($P < 0.001$) from *day 1* to *day 6* and increased significantly ($P < 0.001$) at *day 10* for all strain levels and strain rates. Overall, there was no significant effect of strain level ($P = 0.042$, $\alpha^c = 0.025$) and strain rate ($P = 0.076$) on the difference in phase shifts over the duration of culture ($P = 0.040$, $\alpha^c = 0.025$) (Fig. 6, *right*). A "Bonferroni correction (α^c)" for the value of α was used for this comparison to get a final $\alpha = 0.05$. The median of all the phase shifts was 0.255 radians, with 0.314 radians as the 75th percentile.

Effects of MMP-9 on material properties of native collagen gels. Since it was hypothesized that changes in the mechanical properties of the vascularized constructs may be due, at least in part, to MMP activity on the collagen matrix, we examined the effects of MMP-9 treatment on the mechanical properties of native gels. The posttreatment values for each gel were normalized to its pretreatment values to get a paired "post/pre" ratio. The MMP-9 treatment caused a highly significant reduction (by ~50%; Fig. 7) in the dynamic stiffness of the native collagen gels ($P = 0.001$, $P = 0.003$, $P = 0.003$ with $\alpha = 0.05$ for strain levels of 2, 4, and 6%, respectively). Control groups did not show a significant difference in dynamic stiffness between test times ($P = 0.316$, $P = 0.686$, $P = 0.219$ for strain levels of 2, 4, and 6%, respectively), and the normalized ratio was close to 1.0 (Fig. 7). There were no significant changes in the phase-shift differences for the MMP-9 or control groups.

Quantitative PCR. Gene expression studies were performed to assess the time profile of expression of genes for MMPs, ECM components, cell-ECM interaction genes, and growth factors during the culture period. In general, maximum expression of MMPs occurred at *day 6* of culture, remaining relatively unchanged at *day 10* (Fig. 8, *top left*). There was a significant increase in MMP-2 expression level between *day 1* and *day 6* ($P < 0.001$), *day 1* and *day 10* ($P = 0.002$), and *day 6* and *day 10* ($P = 0.009$). MMP-9 showed a significant increase at *day 6* compared with *day 1* ($P = 0.038$). MMP-13 mRNA was elevated at *day 6* ($P = 0.003$) and *day 10* ($P = 0.002$) compared with the levels at *day 1*. There were no significant effects of culture time on expression levels for MT1-MMP (MMP-14 results not shown), TIMP-1, or TIMP-2.
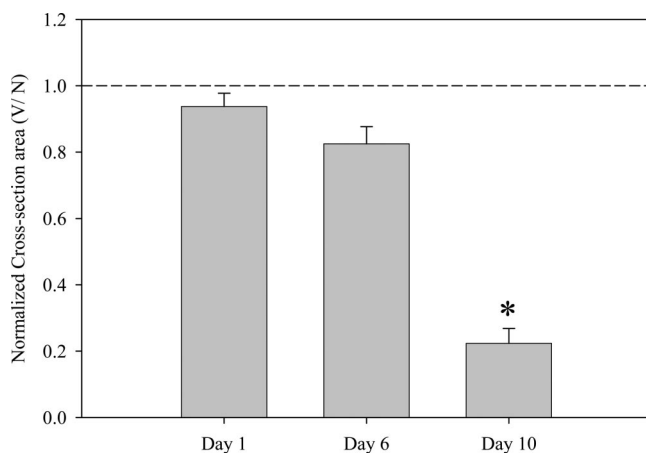

Fig. 4. Effect of culture time on normalized cross-sectional area [ratio of vascularized to native constructs (V/N)]. Values are means ± SE. *There was a significant decrease in cross-sectional area at *day 10* of culture.
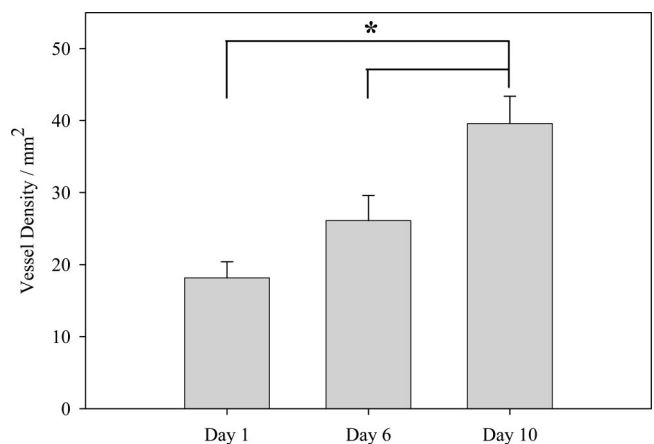

Fig. 5. Effect of culture time on microvessel density. Values are means ± SE. **Day 10* cultures had significantly higher microvessel density than *day 1* and *day 6* cultures.
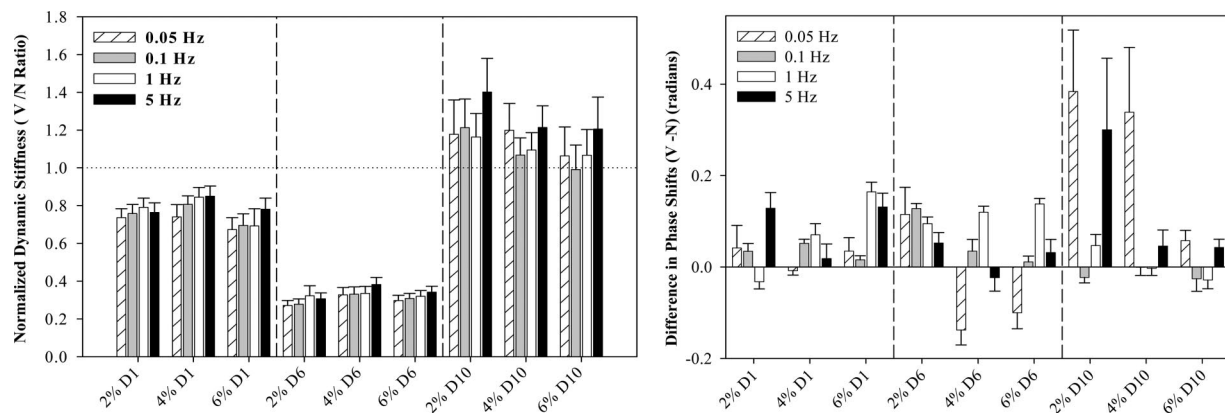
Fig. 6. Results from viscoelastic mechanical testing of vascularized constructs. *Left*: normalized dynamic stiffness as a function of culture time, strain level, and frequency. The normalized stiffness is the ratio of that of the vascularized gels to that of the native constructs at the same time point. *Right*: phase-shift difference as a function of culture time, strain level, and frequency. The difference in phase shift is the phase shift of the vascularized constructs minus the phase shift of the native gels at the same time point (V − N). Values are means ± SE. D1–D10, *days 1–10*, respectively.

Three of the four growth factors did not show a significant change in mRNA levels throughout the culture period (Fig. 8, *bottom right*). Only PDGF showed a significant peak in mRNA on *day 1* of culture ($P = 0.004$ and 0.006 with respect to *days 6* and *10*, respectively), returning to baseline levels by *day 6*.

There were no significant changes in mRNA levels for collagens I, III, or VIII (Fig. 8, *top right*), but there were significant changes in the expression of cell-matrix interaction genes (Fig. 8, *bottom left*). There was a significant upregulation of message for DCN, TNC, and FN with culture time. DCN levels increased through the culture period ($P < 0.001$ for all comparisons), while FN ($P < 0.001$, $P = 0.002$) and TNC ($P < 0.001$ for both cases) mRNA levels at *day 6* and *day 10* were significantly higher than their *day 1* levels. HAS, an anti-angiogenic molecule, was significantly downregulated from its *day 1* levels at both *day 6* and *day 10* ($P = 0.006$, $P < 0.001$).

Proteolytic activity and MMP zymography. We assessed MMP enzyme levels and proteolytic activity in the cultures to determine whether there were temporal differences between gene expression profiles and active enzyme levels. The total

normalized proteolytic activity showed a significant increase on the 6th day compared with both the 1st ($P = 0.011$) and 10th ($P = 0.045$) days of culture (Fig. 9, *first* panel). Figure 9 (*second* and *third* panels) shows the results for one of the two sets of constructs analyzed for specific MMP-2 and MMP-9 activity. Consistent with the gene expression changes, there was an increase in the amount of MMP-2 and MMP-9 protein able to be activated from *day 1* to *day 6*. This was true for both diffusible enzyme (in the media) and nondiffusible enzyme (in the construct). In addition, there was a greater proportion of MMP-2 enzyme to proenzyme in the *day 6* and *day 10* constructs compared with *day 1* constructs (Fig. 9, *fourth* panel). Interestingly, MMP enzyme levels remained elevated in the *day 10* samples, despite the drop in measured overall protease activity. This suggests that the decrease in protease activity is likely due to the activity of protease inhibitors and not reduced MMP protein levels or conversion from the proenzyme to the active enzyme forms.

DISCUSSION

The changes in microvessel density of the vascularized constructs over culture time provide a global picture of the progression of growth and proliferation. There was a continued increase in the microvessel density with increasing culture time (Fig. 5), while phase-contrast micrographs showed that this increase during the early culture periods was due to initial sprouting, followed later by the elongation and anastamosis of new sprouts. By *day 10* of culture, there was a dramatic and significant decrease in construct cross-sectional area to ~20% of that of the nonvascularized control gels (Fig. 4). This result is consistent with the results for many in vitro culture models involving ECs (e.g., Ref. 41), and the cause is an increase in cell-matrix traction forces (38, 43). This reduction in cross-sectional area was readily visible to the naked eye. Despite substantial contraction by the later culture times, the vascularized constructs remained anchored to the attachment posts. When the results for microvessel density and cross-sectional area are considered together, it is clear that the overall increase in microvessel fragment density was due to a combination of microvessel growth and proliferation and compaction of the microvessel constructs.
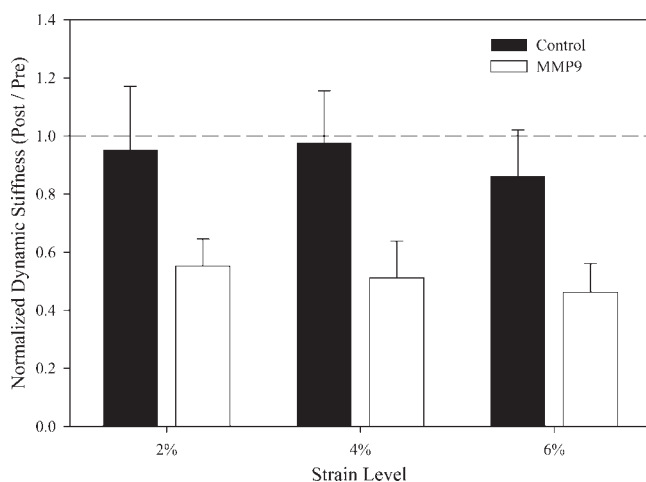

Fig. 7. Effects of matrix metalloproteinase (MMP)-9 on material properties of native collagen gels. Posttreatment data were normalized pairwise to pretreatment data (Post/Pre). Values are means ± SE.
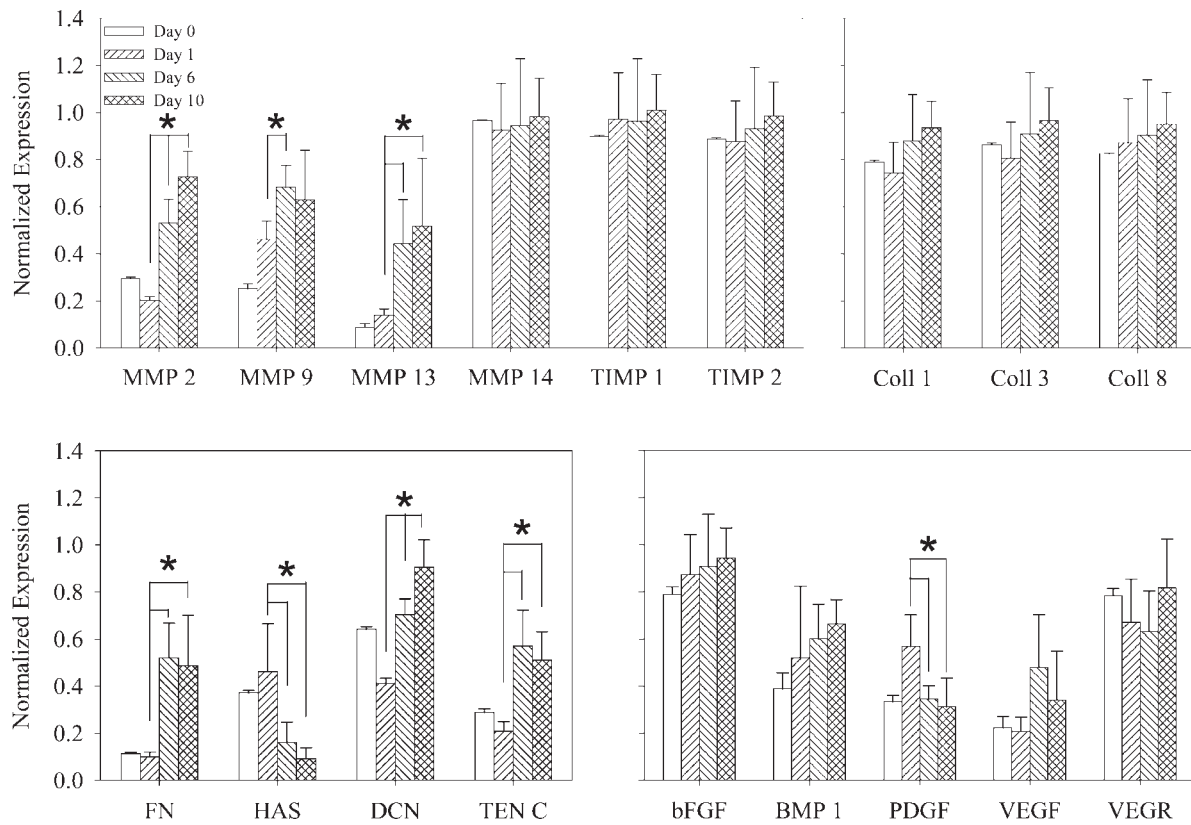
Fig. 8. Gene expression as a function of culture time. *Top left*: MMPs and their inhibitors. *Top right*: collagens (Coll). *Bottom left*: cell-matrix interaction genes. *Bottom right*: growth factors. Values are means ± SD. *Significant differences. See text for details. TIMP, tissue inhibitor of MMP; FN, fibronectin; HAS, hyaluronic acid synthase; DCN, decorin; TEN C, tenascin C; bFGF, basic FGF; BMP, bone morphogenic protein; PDGF, platelet-derived growth factor; VEGF, vascular endothelial growth factor; VEGR, VEGF-receptor.

Cellular remodeling exerts a strong influence on ECM mechanical properties due to matrilysis, cell adhesion, and the resulting compression and reorientation of the ECM. These effects are evident in our results for the dynamics stiffness of the constructs. The dynamic stiffness of the native constructs in this study were comparable to those of our laboratory's earlier study (20). The *day 6* cultures showed a mild reduction in cross-sectional area (Fig. 4), but a significant reduction in dynamics stiffness compared with *day 1* values (Fig. 6). This reduction in stiffness parallels an increase in microvessel density (Fig. 5) and the peaks in proteolytic activity (Fig. 9) and mRNA expression levels for MMPs-2, -9, and -13 (Fig. 8).

Taken together, these results strongly suggest that proteolysis was responsible for the reduction in dynamic stiffness at *day 6* of culture. To confirm that MMP enzymatic degradation could decrease the dynamic stiffness of the collagen constructs, we treated native collagen gels with activated MMP-9 enzyme. MMP-9 treatment resulted in a significant reduction in the dynamic stiffness of the native collagen gels, with a reduction in magnitude that was similar to that observed in the in vitro studies (Fig. 7). These results demonstrate that global MMP activity can reduce the dynamic stiffness of the collagen gels.

Enzyme cleavage sites on collagen have usually been attributed to weaker or susceptible areas in its helical molecular
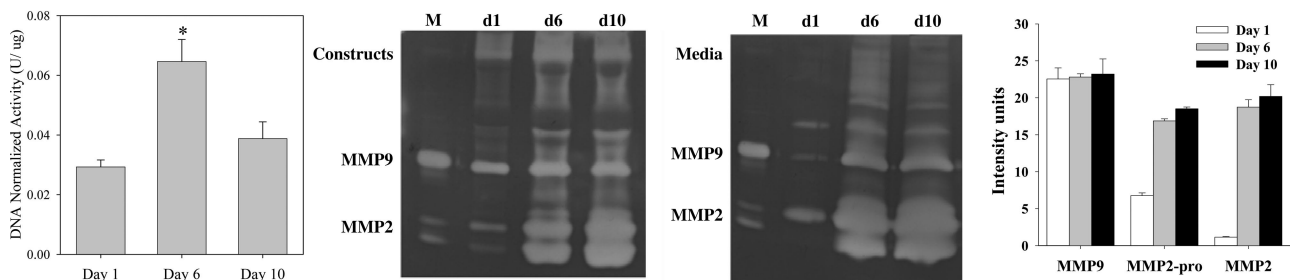
Fig. 9. *First* panel: proteolytic activity combined for the media and tissue lysates, normalized to DNA content. *Significant difference. Values are means ± SE. *Second* and *third* panels: MMP zymography results for the construct lysates (cell/tissue lysates) and media, respectively. Lane labeled "M" represents MMP-9 and MMP-2 standard purified enzymes. Results were obtained at *days 1*, *6*, and *10* (d1, d6, d10, respectively). Both MMP-2 and MMP-9 enzymatic activity were sharply increased at *days 6* and *10*. The two bands for MMP-2 represent a proenzyme form and an enzyme form. *Fourth* panel: densitometric measurements of select band intensities from the two replicate construct experiments.

structure. There are a limited number of cleavage sites available on the native collagen molecule for digestion by eukaryotic collagenases, and this is generally attributed to their specificity of local motifs in a relatively narrow region of the substrate (21). Enzymatic degradation of collagen is thus dependent on the availability of these specific motifs, which may be altered under loading. This has been unequivocally demonstrated by Ruberti and Hallab (28) in a type I/V heterotypic collagen structure of the bovine corneal stroma, where fibrils under low-tensile load were preferentially cleaved by a collagenase (Clostridiopeptidase A). The contraction of vascularized constructs, especially by *day 10*, in turn could lead to a reduced susceptibility to enzymatic digestion, especially by the rat MMPs (as opposed to bacterial enzymes with multiple cleavage sites) and contribute to the increased stiffness observed at *day 10*.

The mechanical measurements for the vascularized constructs at *day 10* demonstrate an increase in normalized dynamic stiffness, even in relation to the *day 1* measurements. This was accompanied by a substantial reduction in cross-sectional area (Fig. 4) and continued increase in microvascular density (Fig. 5). The apparent paradox between high MMP mRNA levels, reduction in construct area, and reduction in observed proteolytic activity can be resolved by considering the effects of syneresis and cell-ECM interactions. As the microvessel fragments contract the gel, they force liquid from the gel. Since dynamic stiffness is normalized by cross-sectional area, a reduction in the fluid phase results in an effective increase in solid-phase fraction. It is likely that better cell-ECM contacts, engineered by the molecules DCN, FN, TNC and HAS, also contribute to the stiffening of the constructs at *day 10*. In addition, FN deposition promotes clustering of focal adhesion complexes, resulting in stronger adhesion of ECs to the matrix, thus increasing the contribution of the active cellular phase to the overall dynamic stiffness of the vascularized constructs. It is also possible that anisotropy induced by gel contraction affected the mechanical properties in these constructs. Studies on matrices with high-aspect ratios and similarly restrained cell-seeded constructs (10) demonstrate a higher level of orientation and associated strength (34, 42) between anchorage posts. The sharp drop in cross-sectional area (Fig. 4) and increased vascular density by *day 10* of culture in the present study might indicate a similar behavior, progressively inducing vascular and collagen orientation along the direction of anchorage. This could have introduced anisotropy to the vascularized constructs and thus increased their stiffness along the direction of anchorage.

The results for gene expression of MMPs, their inhibitors, and protease activity illustrate the progression of the microvessel fragments from a relatively quiescent phenotype immediately after isolation to an invasive phenotype. Normal capillary ECs are quiescent and retained within their investing basement membrane. The switch of ECs to the angiogenic phenotype is marked by increased lytic activity by MMPs (3, 36) and plasminogen activator systems. One of the major roles of MMPs in angiogenesis is collagen cleavage (32, 36), which is a prerequisite for EC invasiveness and angiogenesis (3). MMP-9 may play a significant role in switching to the angiogenic phenotype (1). The significant increases in mRNA levels of gelatinases (MMPs-2, -9) and the major rodent endothelial interstitial collagenase (MMP-13) (3) at *day 6* of culture

support an invasive angiogenic switch. Peak MMP mRNA levels have been found on the 6th day of EC co-cultures with fibroblasts, with a downregulation by the 12th day (30). Our results suggest a switch from a general invasive phase to a more selective invasion at later culture times. This is supported by our data for total proteolytic activity, which peaks at *day 6* and falls at *day 10*. MMP-2 is known to bind native collagen I (44), making this protease an excellent effector of focal matrix degradation/remodeling.

MMP-2 and MT1-MMP are normally endogenously expressed by microvessel ECs in culture and increase with formation of "sprout"-like outgrowths, especially from confluent monolayers (15, 30). The constant level of MT1-MMP over 10 days of culture in the present study suggests either that MT1-MMP is not the bottleneck in the activation of MMP-2, or that invasion is more widespread than just local proteolysis. However, considering the MMP activity over the entire culture period, it is seen that, on *day 10*, only MMP-2 continues to increase significantly, while MMP-9 and -13 levels do not differ significantly from *day 6* levels. In addition, there were no significant changes in the mRNA levels of TIMPs over the culture period. Our results for TIMP-2 expression are consistent with those of another study examining in vitro angiogenesis from isolated ECs in a collagen matrix (15).

Increases in gene expression for molecules responsible for cell-ECM adhesion and interaction are characteristic of the proliferation phase of angiogenesis. There were significant increases in mRNA levels for FN, DCN, and TNC at *days 6* and *10* of culture, with a concomitant reduction in HAS, an enzyme catalyzing the synthesis of the glycosaminoglycan hyaluronan. DCN, localized around endothelial cords and cavities, is causally involved in capillary formation and reduction of apoptosis (29, 31). It inhibits cell binding to collagen and FN and promotes migration, which, in turn, may be responsible for cord-like alignment (7, 35). Similar roles have been suggested for TNC (19, 46). Hyaluronan has an angiogenesis-inhibiting role (37), which explains the downregulation of HAS over culture time in our study. Matricellular proteins like TNC and DCN modulate EC-ECM interaction and regulate deadhesion and intermediate adhesion steps, favoring motility and reducing anoikis (22). It is interesting to note that the plateau of TNC mRNA level noted at *day 10* follows the plateauing effect of TNC on tube lengthening and EC migration (4).

This study examined expression of fibroblast growth factor (basic FGF), PDGF, VEGF and its receptor (VEGF-R), and bone morphogenic protein-1, all of which have been linked to angiogenesis. Overall, the results for growth factor gene expression indicate a highly proliferative phenotype. The initiation of angiogenesis depends on VEGF, while PDGF is necessary for maintenance and to prevent dissociation of pericytes from ECs during angiogenesis (1, 2, 8). Biological functions of VEGF are transduced by VEGF-R2, a tyrosine kinase receptor expressed predominantly on ECs (5). VEGF receptors are predominantly distributed on adult rat ECs and expressed even on nonangiogenic vessels with detectable VEGF mRNA levels (1, 17). VEGF is highly inducible by hypoxia and serum (12). PDGF showed a significant increase on the 1st day of culture, while the others did not demonstrate a significant increase. This result is consistent with studies of the culture of isolated ECs (18). VEGF production by a tissue or group of cells may thus serve as an indicator for requirement of increased vascu-

lature and set up chemotaxis to promote angiogenesis, with ECs not being a major source of VEGF (8). The difference in growth factor profiles may be attributed to the difference in angiogenesis from formed vascular elements and EC cultures in their requirement of growth factors.

In summary, the results of this study demonstrate that angiogenesis in vitro can have dramatic effects on the material properties of a substrate material through the mechanisms of matrilysis, syneresis, and consolidation/compaction. Questions that remain to be addressed include the relative contribution of local vs. global MMP enzymatic degradation and the influence of mechanical boundary conditions and mechanical loading on the dependent variables investigated in this study. It is thus evident that a finely regulated relationship exists between angiogenesis, the ECM, and its mechanical properties.

REFERENCES

1. **Bergers G, Brekken R, McMahon G, Vu TH, Itoh T, Tamaki K, Tanzawa K, Thorpe P, Itohara S, Werb Z, Hanahan D.** Matrix metalloproteinase-9 triggers the angiogenic switch during carcinogenesis. *Nat Cell Biol* 2: 737–744, 2000.
2. **Brill A, Dashevsky O, Rivo J, Gozal Y, Varon D.** Platelet-derived microparticles induce angiogenesis and stimulate post-ischemic revascularization. *Cardiovasc Res* 67: 30–38, 2005.
3. **Burbridge MF, Coge F, Galizzi JP, Boutin JA, West DC, Tucker GC.** The role of the matrix metalloproteinases during in vitro vessel formation. *Angiogenesis* 5: 215–226, 2002.
4. **Castellon R, Caballero S, Hamdi HK, Atilano SR, Aoki AM, Tarnuzzer RW, Kenney MC, Grant MB, Ljubimov AV.** Effects of tenascin-C on normal and diabetic retinal endothelial cells in culture. *Invest Ophthalmol Vis Sci* 43: 2758–2766, 2002.
5. **Claesson-Welsh L.** Signal transduction by vascular endothelial growth factor receptors. *Biochem Soc Trans* 31: 20–24, 2003.
6. **Curry TE Jr, Dean DD, Woessner JF Jr, LeMaire WJ.** The extraction of a tissue collagenase associated with ovulation in the rat. *Biol Reprod* 33: 981–991, 1985.
7. **de Lange Davies C, Melder JR, Munn LL, Mouta-Carreira C, Jain KR, Boucher Y.** Decorin inhibits endothelial migration and tube-like structure formation: role of thrombospondin-1. *Microvasc Res* 62: 26–42, 2001.
8. **Dvorak HF.** Vascular permeability factor/vascular endothelial growth factor: a critical cytokine in tumor angiogenesis and a potential target for diagnosis and therapy. *J Clin Oncol* 20: 4368–4380, 2002.
9. **Dye J, Lawrence L, Linge C, Leach L, Firth J, Clark P.** Distinct patterns of microvascular endothelial cell morphology are determined by extracellular matrix composition. *Endothelium* 11: 151–167, 2004.
10. **Eastwood M, Mudera VC, McGrouther DA, Brown RA.** Effect of precise mechanical loading on fibroblast populated collagen lattices: morphological changes. *Cell Motil Cytoskeleton* 40: 13–21, 1998.
11. **Eliceiri BP, Cheresh DA.** The role of alphav integrins during angiogenesis. *Mol Med* 4: 741–750, 1998.
12. **Enholm B, Paavonen K, Ristimaki A, Kumar V, Gunji Y, Klefstrom J, Kivinen L, Laiho M, Olofsson B, Joukov V, Eriksson U, Alitalo K.** Comparison of VEGF, VEGF-B, VEGF-C and Ang-1 mRNA regulation by serum, growth factors, oncoproteins and hypoxia. *Oncogene* 14: 2475–2483, 1997.
13. **Findley NW, Lai SJ, Onaran K.** *Creep and Relaxation of Nonlinear Viscoelastic Materials: With an Introduction to Linear Viscoelasticity.* Amsterdam: North Holland Publishing, 1976.
14. **Fournier N, Doillon CJ.** In vitro angiogenesis in fibrin matrices containing fibronectin or hyaluronic acid. *Cell Biol Int* 16: 1251–1263, 1992.
15. **Haas TL, Davis SJ, Madri JA.** Three-dimensional type I collagen lattices induce coordinate expression of matrix metalloproteinases MT1-MMP and MMP-2 in microvascular endothelial cells. *J Biol Chem* 273: 3604–3610, 1998.
16. **Hoying JB, Boswell CA, Williams SK.** Angiogenic potential of microvessel fragments established in three-dimensional collagen gels. *In Vitro Cell Dev Biol Anim* 32: 409–419, 1996.
17. **Jakeman LB, Winer J, Bennett GL, Altar CA, Ferrara N.** Binding sites for vascular endothelial growth factor are localized on endothelial cells in adult rat tissues. *J Clin Invest* 89: 244–253, 1992.
18. **Kallmann BA, Wagner S, Hummel V, Buttmann M, Bayas A, Tonn JC, Rieckmann P.** Characteristic gene expression profile of primary human cerebral endothelial cells. *FASEB J* 16: 589–591, 2002.
19. **Kim CH, Bak KH, Kim YS, Kim JM, Ko Y, Oh SJ, Kim KM, Hong EK.** Expression of tenascin-C in astrocytic tumors: its relevance to proliferation and angiogenesis. *Surg Neurol* 54: 235–240, 2000.
20. **Krishnan L, Weiss JA, Wessman MD, Hoying JB.** Design and application of a test system for viscoelastic characterization of collagen gels. *Tissue Eng* 10: 241–252, 2004.
21. **Lecroisey A, Keil B.** Differences in the degradation of native collagen by two microbial collagenases. *Biochem J* 179: 53–58, 1979.
22. **Murphy-Ullrich JE.** The de-adhesive activity of matricellular proteins: is intermediate cell adhesion an adaptive state? *J Clin Invest* 107: 785–790, 2001.
23. **Pepper MS.** Role of the matrix metalloproteinase and plasminogen activator-plasmin systems in angiogenesis. *Arterioscler Thromb Vasc Biol* 21: 1104–1117, 2001.
24. **Reno C, Marchuk L, Sciore P, Frank CB, Hart DA.** Rapid isolation of total RNA from small samples of hypocellular, dense connective tissues. *Biotechniques* 22: 1082–1086, 1997.
25. **Risau W.** Mechanisms of angiogenesis. *Nature* 386: 671–674, 1997.
26. **Rooney P, Kumar S.** Inverse relationship between hyaluronan and collagens in development and angiogenesis. *Differentiation* 54: 1–9, 1993.
27. **Rozen S, Skaletsky H.** Primer3 on the WWW for general users and for biologist programmers. *Methods Mol Biol* 132: 365–386, 2000.
28. **Ruberti JW, Hallab NJ.** Strain-controlled enzymatic cleavage of collagen in loaded matrix. *Biochem Biophys Res Commun* 336: 483–489, 2005.
29. **Schonherr E, O'Connell BC, Schittny J, Robenek H, Fastermann D, Fisher LW, Plenz G, Vischer P, Young MF, Kresse H.** Paracrine or virus-mediated induction of decorin expression by endothelial cells contributes to tube formation and prevention of apoptosis in collagen lattices. *Eur J Cell Biol* 78: 44–55, 1999.
30. **Schonherr E, Schaefer L, O'Connell BC, Kresse H.** Matrix metalloproteinase expression by endothelial cells in collagen lattices changes during co-culture with fibroblasts and upon induction of decorin expression. *J Cell Physiol* 187: 37–47, 2001.
31. **Schonherr E, Sunderkotter C, Schaefer L, Thanos S, Grassel S, Oldberg A, Iozzo RV, Young MF, Kresse H.** Decorin deficiency leads to impaired angiogenesis in injured mouse cornea. *J Vasc Res* 41: 499–508, 2004.
32. **Seandel M, Noack-Kunnmann K, Zhu D, Aimes RT, Quigley JP.** Growth factor-induced angiogenesis in vivo requires specific cleavage of fibrillar type I collagen. *Blood* 97: 2323–2332, 2001.
33. **Shepherd BR, Chen HY, Smith CM, Gruionu G, Williams SK, Hoying JB.** Rapid perfusion and network remodeling in a microvascular construct after implantation. *Arterioscler Thromb Vasc Biol* 24: 898–904, 2004.
34. **Shi Y, Rittman L, Vesely I.** Novel geometries for tissue-engineered tendonous collagen constructs. *Tissue Eng* 12: 2601–2609, 2006.
35. **Spring J, Beck K, Chiquet-Ehrismann R.** Two contrary functions of tenascin: dissection of the active sites by recombinant tenascin fragments. *Cell* 59: 325–334, 1989.
36. **Stupack GD, Cheresh AD.** ECM remodeling regulates angiogenesis: endothelial integrins look for new ligands. *Sci STKE* 119: PE7, 2002.
37. **Tempel C, Gilead A, Neeman M.** Hyaluronic acid as an anti-angiogenic shield in the preovulatory rat follicle. *Biol Reprod* 63: 134–140, 2000.
38. **Tranqui L, Tracqui P.** Mechanical signalling and angiogenesis. The integration of cell-extracellular matrix couplings. *C R Acad Sci III* 323: 31–47, 2000.
39. **Vailhe B, Ronot X, Tracqui P, Usson Y, Tranqui L.** In vitro angiogenesis is modulated by the mechanical properties of fibrin gels and is related to alpha(v)beta3 integrin localization. *In Vitro Cell Dev Biol Anim* 33: 763–773, 1997.
40. **Vandesompele J, De Preter K, Pattyn F, Poppe B, Van Roy N, De Paepe A, Speleman F.** Accurate normalization of real-time quantitative RT-PCR data by geometric averaging of multiple internal control genes. *Genome Biol* 3: 0034.1–0034.11, 2002.

41. **Vernon RB, Sage EH.** Contraction of fibrillar type I collagen by endothelial cells: a study in vitro. *J Cell Biochem* 60: 185–197, 1996.
42. **Vesely I.** Heart valve tissue engineering. *Circ Res* 97: 743–755, 2005.
43. **Wakatsuki T, Kolodney M, Zahalak G, Elson E.** Cell mechanics studied by a reconstituted model tissue. *Biophys J* 79: 2353–2368, 2000.
44. **Wallon UM, Overall CM.** The hemopexin-like domain (C domain) of human gelatinase A (matrix metalloproteinase-2) requires Ca^{2+} for fibronectin and heparin binding. Binding properties of recombinant gelatinase A C domain to extracellular matrix and basement membrane components. *J Biol Chem* 272: 7473–7481, 1997.
45. **Weeks JG, Halme J, Woessner JF Jr.** Extraction of collagenase from the involuting rat uterus. *Biochim Biophys Acta* 445: 205–214, 1976.
46. **Zagzag D, Shiff B, Jallo GI, Greco MA, Blanco C, Cohen H, Hukin J, Allen JC, Friedlander DR.** Tenascin-C promotes microvascular cell migration and phosphorylation of focal adhesion kinase. *Cancer Res* 62: 2660–2668, 2002.